Crystal structure of two quaternary complexes of dethiobiotin synthetase, enzyme-MgADP-AlF 3 -diaminopelargonic acid and enzyme-MgADP-dethiobiotin-phosphate; implications for catal...

ARTICLE *in* PROTEIN SCIENCE · DECEMBER 1998

Impact Factor: 2.85 · DOI: 10.1002/pro.5560071209 · Source: PubMed

Protein Science (1998), 7:2560–2566. Cambridge University Press. Printed in the USA.

Crystal structure of two quaternary complexes of dethiobiotin synthetase, enzyme-MgADP-AlF_3-diaminopelargonic acid and enzyme-MgADP-dethiobiotin-phosphate; implications for catalysis

HELENA KÄCK,[1] JENNY SANDMARK,[1] KATHARINE J. GIBSON,[2] GUNTER SCHNEIDER,[1] AND YLVA LINDQVIST[1]

[1]Division of Molecular Structural Biology, Department of Medical Biochemistry and Biophysics, Karolinska Institutet, 171 77 Stockholm, Sweden
[2]DuPont Central Research & Development, Experimental Station, P.O. Box 80328, Wilmington, Delaware 19880-0328

(RECEIVED July 29, 1998; ACCEPTED September 4, 1998)

Abstract

The crystal structures of two complexes of dethiobiotin synthetase, enzyme-diaminopelargonic acid-MgADP-AlF_3 and enzyme-dethiobiotin-MgADP-Pi, respectively, have been determined to 1.8 Å resolution. In dethiobiotin synthetase, AlF_3 together with carbamylated diaminopelargonic acid mimics the phosphorylated reaction intermediate rather than the transition state complex for phosphoryl transfer. Observed differences in the binding of substrate, diaminopelargonic acid, and the product, dethiobiotin, suggest considerable displacements of substrate atoms during the ring closure step of the catalytic reaction. In both complexes, two metal ions are observed at the active site, providing evidence for a two-metal mechanism for this enzyme.

Keywords: aluminum fluoride; biotin synthesis; enzyme mechanism; phosphoryl transfer; transition state analogue

Dethiobiotin synthetase (DTBS) is the penultimate enzyme in the biotin synthesis pathway in micro-organisms (Eisenberg, 1973; Gloeckler et al., 1990) and plants (Baldet et al., 1993). The enzyme catalyzes the conversion of 7,8-diaminopelargonic acid (DAPA) to dethiobiotin (DTB) using carbon dioxide and MgATP as additional substrates (Krell & Eisenberg, 1970). The enzyme subunit, consisting of 224 amino acids, folds into a single α/β domain, with a central seven-stranded parallel β-sheet (Alexeev et al., 1994; Huang et al., 1994). The active form of the enzyme is a homodimer and the two active sites are located at the interface between the subunits, approximately 25 Å away from each other. Each active site is built up from residues of predominantly one subunit. However, the hydrophobic carbon tail of the substrate, DAPA, extends across the subunit-subunit interface and its terminal carboxyl group interacts with residues from the second subunit (Alexeev et al., 1995; Huang et al., 1995).

Reprint requests to: Ylva Lindqvist, Division of Molecular Structural Biology, Department of Medical Biochemistry and Biophysics, Karolinska Institutet, 171 77 Stockholm, Sweden; e-mail: Ylva.alfa.mbb.ki.se.

Abbreviations: DAPA, diaminopelargonic acid; DTB, dethiobiotin; DTBS, dethiobiotin synthetase; MPD, 2-methyl-2,4-pentanediol.

The first step in the DTBS reaction, which can occur in the absence of MgATP, is the carbamylation of the N7-nitrogen of DAPA through reaction with CO_2 (Alexeev et al., 1995; Gibson et al., 1995; Huang et al., 1995) (Fig. 1). Subsequently, one of the carbamate oxygens attacks the γ-phosphorus atom of MgATP, which results in the formation of a mixed carbamic-phosphoric acid anhydride and MgADP (Baxter & Baxter, 1994; Gibson, 1997; Käck et al., 1998). This step is followed by closure of the ureido ring through nucleophilic attack of the eight-amino nitrogen on the activated carbonyl group of the mixed anhydride. The reaction, which may proceed through a tetrahedral intermediate, leads to formation of DTB and inorganic phosphate. Several of the proposed mechanistic steps are supported by high resolution crystal structures (Alexeev et al., 1995; Huang et al., 1995; Käck et al., 1998). A unique feature in the mechanism of DTBS is the stabilization of one of the reaction intermediates, the carbamic-phosphoric acid anhydride by a second Mg^{2+} ion that binds to the active site, probably after phosphoryl transfer has occurred (Käck et al., 1998).

To further characterize this reaction mechanism we have extended the crystallographic analysis. We report here the high resolution structures of the DTBS-MgADP-DAPA-AlF_3 and the DTBS-MgADP-DTB-Pi complexes. The crystal structure of the

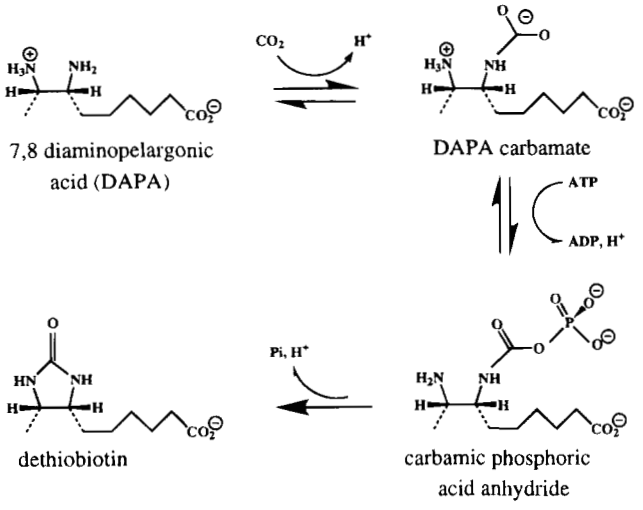

Fig. 1. Reaction scheme for DTBS.

DTBS-MgADP-DAPA-AlF_3 complex provides additional evidence for the formation of a mixed carbamic-phosphoric acid anhydride as an intermediate in the catalytic reaction. It also shows that in DTBS, AlF_3 together with DAPA carbamate mimics the phosphorylated reaction intermediate, rather than the transition state for phosphoryl transfer. The crystal structure of the enzyme-product complex provides structural insights into the second half of the catalytic reaction and suggests considerable displacements of substrate atoms during the ring closure step.

Results

For both complexes, the overall structure of the enzyme is well-defined with continuous electron density for the polypeptide chain except for a disordered loop region (residues 208–212). Ramachandran plots show 89% of the residues in the most favorable regions of the Φ, Ψ space, and no residues are found in the unfavorable regions. The overall structure of the enzyme in the two complexes is very similar to the structure of the ternary complex DTBS-MgADP-DAPA (Huang et al., 1995), with RMS deviations (RMSDs) for all Cα atoms of 0.35 Å for the DTBS-MgADP-DAPA-AlF_3 complex, and 0.36 Å for the DTBS-MgADP-DTB-Pi complex, respectively.

Structure of the DTBS-MgADP-DAPA-AlF_3 complex

The electron density map at 1.8 Å resolution for the DTBS-MgADP-AlF_3 complex showed clear electron density for the bound substrates (Fig. 2A) and allowed an unambiguous assignment of the positions of MgADP and carbamylated DAPA at the active site (Fig. 3A). After modeling bound MgADP and the carbamylated DAPA in the active site, there was significant residual difference in electron density situated between one of the carbamate oxygen atoms of DAPA and the β-phosphate group of MgADP (Fig. 2A). This electron density, found close to the position of the γ-phosphate group of MgATP when bound to DTBS (Käck et al., 1998), is interpreted as bound AlF_3. The shape of the density and the observed distances to surrounding substrate and protein atoms suggest that in DTBS, AlF_3 is bound not in a planar fashion but with tetrahedral coordination geometry. The Al^{3+} ion is forming a coordination bond (2.2 Å) to the DAPA carbamate oxygen, and to three fluoride ions. The distance of the Al^{3+} ion to the plane of the three fluoride ions is 0.6 Å. There is no coordination to MgADP; the closest oxygen atom of the β-phosphate of MgADP is 3.2 Å from the Al^{3+} ion. One fluoride ion interacts through hydrogen bonds with the side chains of Thr11 and Lys15, a second fluoride is close (2.0 Å) to the Mg^{2+} ion of MgADP (site I Mg^{2+}) (Fig. 3A). The third fluoride interacts with the N8 nitrogen of DAPA and is also coordinated to a second Mg^{2+} ion (site II Mg^{2+}). This second metal binding site in DTBS, which is created entirely by bound substrates and does not involve protein atoms in any way, was recently identified in the structure of the complex of DTBS and the phosphorylated reaction intermediate (Käck et al., 1998).

The positions of the bound MgADP and DAPA in the DTBS-MgADP-DAPA-AlF_3 complex superpose well with those found in other complexes of DTBS, for instance the DTBS-DAPA binary complex or the DTBS-MnADP-DAPA ternary complex (Huang et al., 1995). The interactions between the bound substrates and amino acid residues of the enzyme are identical to those described previously. Furthermore, a superposition of the DTBS-MgADP-DAPA-AlF_3 complex described here with the structure of DTBS with the phosphorylated DAPA carbamate (Käck et al., 1998) shows that the atomic positions of this intermediate and the DAPA carbamate-AlF_3 are identical, within the error of the X-ray analysis.

The product complex; DTBS-MgADP-DTB-Pi

The bound products in the DTBS-MgADP-DTB-Pi complex showed up clearly in the initial difference density map (Fig. 2B). ADP, DTB and the two Mg^{2+} ions could be located unambiguously (Fig. 3B). The interactions of the MgADP molecule with active site residues are identical to those seen in other DTBS-MgADP complexes (Huang et al., 1995). In addition, a phosphate ion is bound at the active site, close to the β-phosphate group of MgADP. It is bound in the same way as the phosphate group in the phosphorylated reaction intermediate (Käck et al., 1998) and is held into position through interactions with the main chain nitrogen of Gly118, the side chains of Thr11, Lys15, and Lys37 and to both metal ions at the active site.

Overall, the binding of the product, DTB, is similar to that of the substrate, DAPA. In both cases, the terminal carboxyl group forms hydrogen bonds to the main-chain nitrogen atoms of residues 150 and 153, respectively, and to the side chain of Tyr187. All these residues are from the second subunit. The hydrophobic chain then spans the space between the two subunits and packs against residues from the loops after strand β3 and β4. However, bound DTB is significantly more bent than DAPA, in particular between atoms C2 and C4 (Fig. 4). This conformational difference is most likely due to the space requirements at the other end of the molecule after ring formation. Like the carbamylated diamine of DAPA, the ureido ring of DTB binds in a rather open pocket, close to ADP. The binding pocket is formed by residues from three loop regions, Ala40–Gly42, Glu78–Pro82, and Gly116–Gly118. However, an important difference between the two structures is that the side chain of Ser41 is hydrogen bonded to N7 of DAPA, while both the main-chain oxygen and the side-chain hydroxyl group of this residue are hydrogen bonded to N8 in DTB. The N7-nitrogen atom of DTB does not form any interactions with the protein. The carbonyl oxygen atom of the ureido ring is within hydrogen bonding dis-

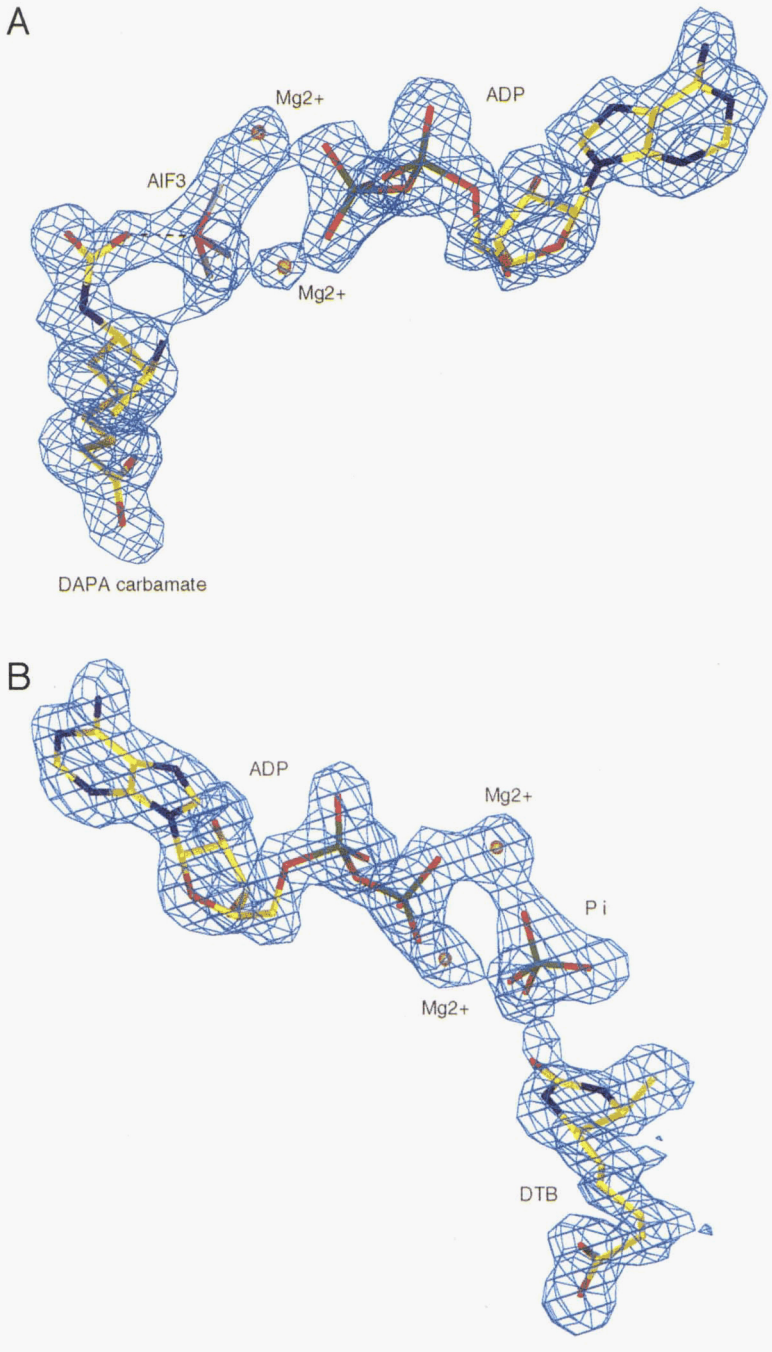

Fig. 2. Initial difference electron density (contoured at 3σ) at the active site in **(A)** the DTBS-MgADP-DAPA-AlF_3 and **(B)** the DTBS-MgADP-DTB-Pi complex.

tance to one of the oxygen atoms of the phosphate ion, indicating that this phosphate oxygen is protonated.

Discussion

AlF_3 mimics the phosphorylated reaction intermediate rather than the transition state

In a number of structural studies, AlF_3 has been used as a transition state analogue in phosphoryl transfer reactions (Coleman et al., 1994; Sondek et al., 1994; Fischer et al., 1995; Scheffstek et al., 1997; Schlichting & Reinstein, 1997; Xu et al., 1997). In these cases, AlF_3 is bound as a planar AlF_3 or AlF_4^- ion with oxygen atoms of the leaving group (in all cases an oxygen atom from the β-phosphate group of a nucleotide) and the attacking nucleophile at the axial positions of a pentagonal or octahedral coordination sphere. In particular, the complexes with pentagonal coordination are considered close mimics of the transition state for phosphoryl transfer (Fig. 5A). In DTBS, the observed coordination geometry is tetrahedral. Tetrahedral coordination of Al^{3+} has been described

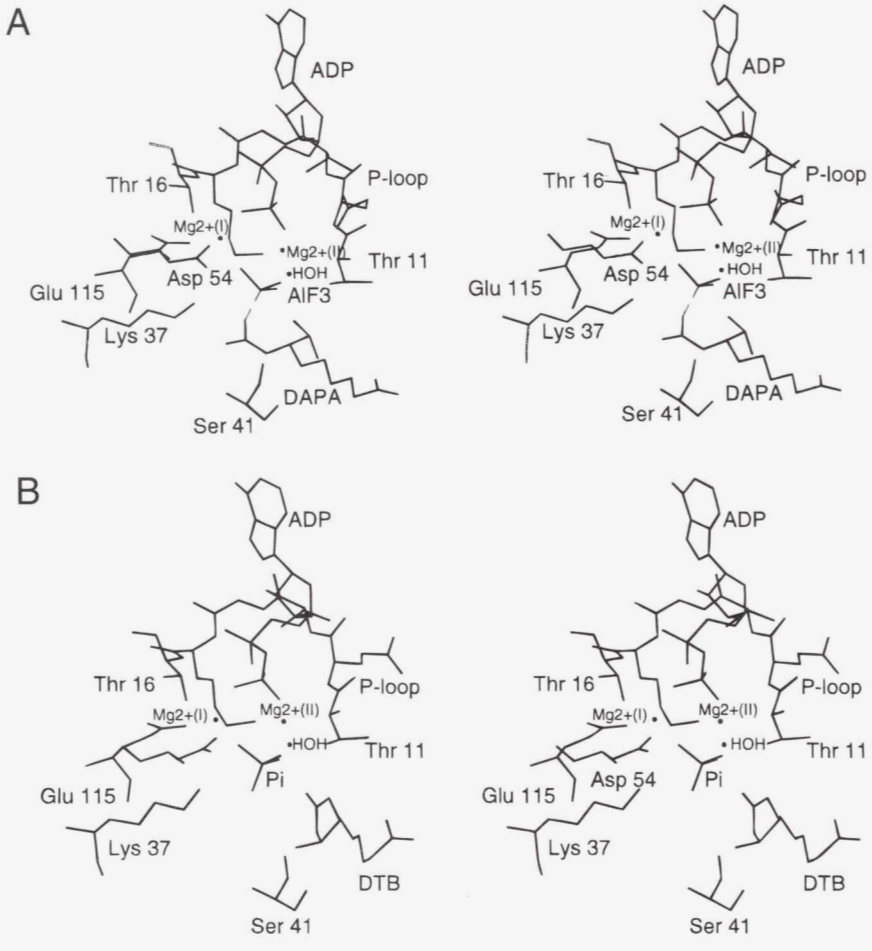

Fig. 3. Stereo view of the active sites in **(A)** the DTBS-MgADP-DAPA-AlF_3 and **(B)** the DTBS-MgADP-DTB-Pi complex.

for the tetrafluoroaluminate anion, both in crystalline form and in solution (Herron et al., 1993). In fact, the observed coordination geometry of AlF_3 is similar to the binding of BeF_3^- observed in the complex with nucleoside diphosphate kinase and MgADP (Xu et al., 1997).

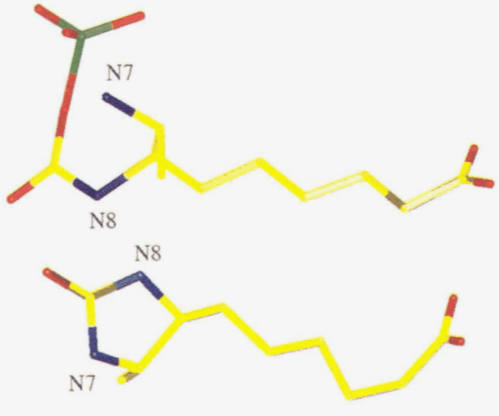

Fig. 4. The reaction intermediate (above) and the product (below) in the same view illustrating the different orientations of the two molecules at the active site of DTBS.

Tetrahedral coordination around the Al^{3+} implies that in DTBS, AlF_3 mimics the phosphorylated reaction intermediate (Fig. 5B,C), formed after phosphoryl transfer rather than the transition state of the reaction. Consistent with this conclusion, the structures of the quaternary complexes DTBS-MgADP-DAPA-AlF_3 and DTBS-MgADP-carbamic phosphoric anhydride are indistinguishable. This difference in behavior of AlF_3, compared to complexes of this compound with other enzymes catalyzing phosphoryl transfer, might be caused by the two Mg^{2+} ions bound to DTBS. Structural and kinetic data indicate that in DTBS phosphoryl transfer very likely proceeds through a similar transition state as in related enzymes, and that the site II Mg^{2+} ion probably enters the reaction pathway after the transfer step. After phosphoryl transfer, the intermediate is stabilized by coordination to this second metal ion. One of the oxygen atoms involved in this metal coordination is the former β,γ bridging oxygen atom of ATP. Participation of this oxygen atom in the ligand sphere of the site II Mg^{2+} ion could possibly decrease its affinity for AlF_3 thus preventing coordination to the Al^{3+} ion.

The ring closure step involves substantial conformational changes of the substrate

There is now compelling biochemical (Gibson, 1997) and structural (Käck et al., 1998) evidence that the mixed carbamic phos-

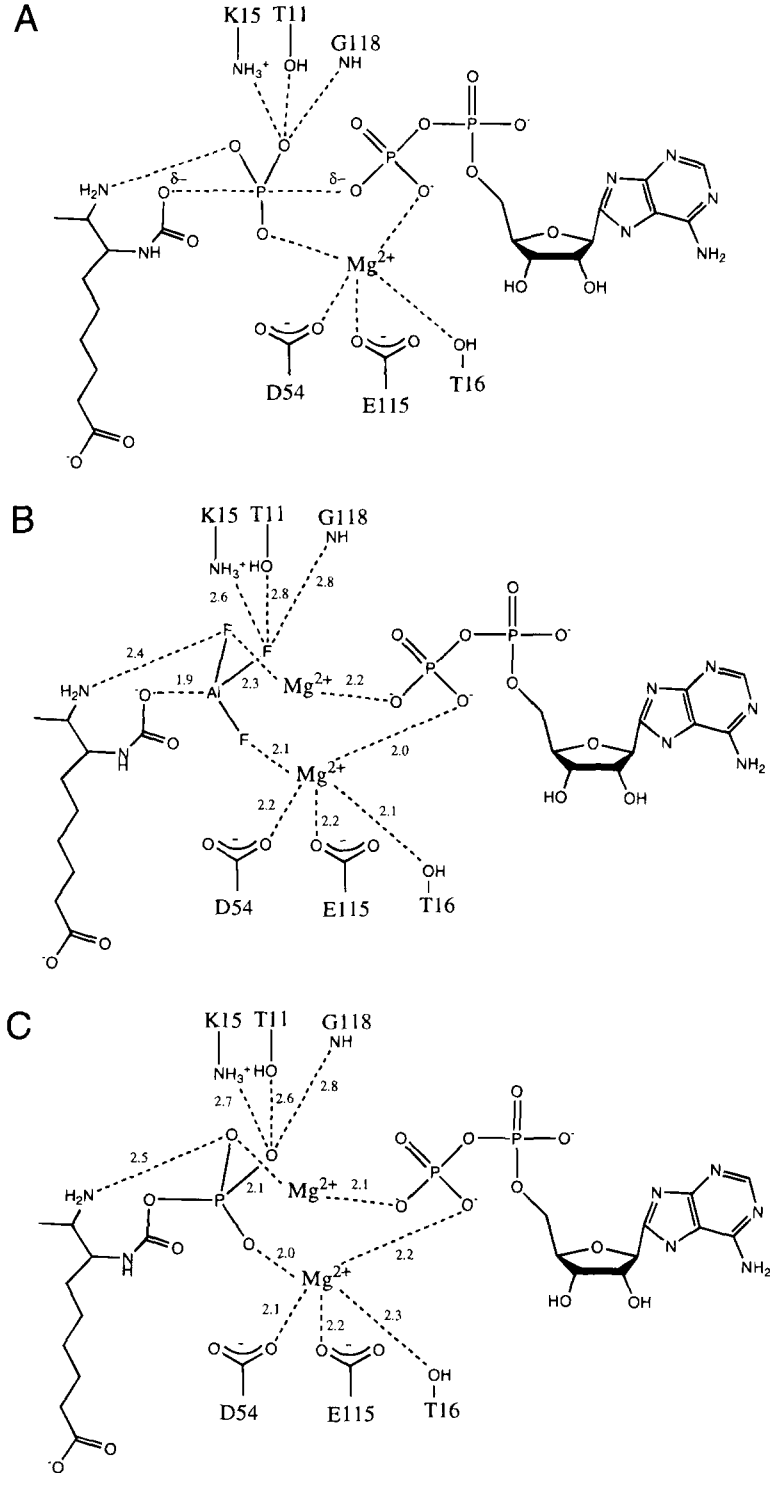

Fig. 5. Schematic view of the active site of DTBS in the (**A**) proposed transition state for phosphoryl transfer, (**B**) the observed DTBS-MgADP-DAPA-AlF_3, and (**C**) in the observed DTBS-MgADP-carbamic phosphoric anhydride complex.

phoric anhydride derivative of DAPA is one of the central intermediates in the catalytic reaction of DTBS. After the formation of this intermediate, the reaction is thought to proceed by nucleophilic attack of the N8 nitrogen atom of the intermediate on the carbonyl carbon, leading to ring closure and release of the phosphate group. Based on the structure of the product complex, several conclusions concerning these steps of the reaction can be made.

The position of the released phosphate group remains unchanged when compared to the positions of the phosphate group in

the intermediate and of the AlF_3 group in the analog of this reaction intermediate. This suggests that during the ring closure step the phosphate is held in place by the many strong interactions with protein atoms and metal ions and therefore does not change its position. Further, the positions of the protein amino acid residues before and after the cyclization step coincide well. However, the phosphorylated intermediate undergoes substantial structural changes when DTB is formed. The chain of DTB is strongly bent compared to that of DAPA, the hydrogen bond between the hydroxyl group of Ser41 and N7 in the mixed anhydride (Käck et al., 1998) has been broken and a new interaction is formed between this residue and the N8 nitrogen in the product so that the positions of the nitrogen atoms are almost interchanged (Fig. 4). N8 and the C9 methyl group shift by approximately 3 Å and N7 moves 2.5 Å. At the same time the plane of the ureido ring is turned almost 180 degrees away from the plane formed by the nitrogen atoms and the connecting carbons in the carbamic-phosphoric acid anhydride (Fig. 4). The structure around the active site seems rather stationary while the substrate changes dramatically. This suggests either a rather rigid active site during the cyclization or that only transient changes in the protein accompany ring formation. Our data are consistent with either alternative.

Formation of a tetrahedral intermediate requires deprotonation of the N8 amino group to form a nucleophile. The data suggest two possible candidates for the needed base. One candidate is a phosphate oxygen of the mixed anhydride. This oxygen atom is 2.5 Å from the N8 nitrogen of DAPA in both the complex with the reaction intermediate (Käck et al., 1998) or its AlF_3 analogue. The oxygen atom is also a ligand to the site II Mg^{2+} ion. The structure of the product complex indicates a hydrogen bond between the carbonyl oxygen of the ureido ring and the phosphate oxygen atom (distance 2.6 Å), suggesting that it is indeed protonated at this state of the reaction, in spite of its coordination to the Mg^{2+} ion. Another candidate is the water molecule which is observed close to the N8 nitrogen atom. This water molecule is within hydrogen bonding distance to the phosphate oxygen and is also within the coordination sphere of the site II Mg^{2+} ion (Fig. 3). As an attack on the carbamyl carbon proceeds, it is possible that the negative charge developing at the carbamyl oxygen is stabilized by the side chain of Lys37, since the ϵ-amino nitrogen is within hydrogen bonding distance of this oxygen atom. Consistent with this idea, replacement of Lys37, by leucine or glutamine resulted in a mutant enzyme severely impaired in catalytic activity, with a 100-fold decrease in k_{cat} (Yang et al., 1997)

Materials and methods

Materials

Purification of dethiobiotin synthetase from an overexpressing strain of *Escherichia coli* was carried out as described (Gibson et al., 1995). ADP was purchased from Boehringer Mannheim (Germany) and dethiobiotin from Sigma-Aldrich Chemie GmbH (Germany). DAPA was prepared as described (Gibson et al., 1995).

Crystallization and data collection

DTBS was crystallized using the hanging-drop method. Five microliters of the well solution, containing 100 mM $Mg(CH_3COO)_2$ or $MgCl_2$, 9–11% polyethylene glycol 8000 and 100 mM cacodylate buffer at pH 6.5 were mixed with 2 μL protein solution (30 mg/mL) and left to equilibrate. Crystals grew within a week at 20 °C.

The DTBS-MgADP-DAPA-AlF_3 complex was prepared by first incubating crystals of DTBS in a solution containing 10 mM $Mg(CH_3COO)_2$, 30 mM $NaHCO_3$, 50 mM hepes pH 7.5, 10 mM DAPA, and 22.5% PEG 8000. After 45 min the crystals were transferred to the same mother solution, which in addition con-

Table 1. *Details of data collection and refinement*[a]

	AlF_3 complex	Product complex
Space group	C2	C2
Cell dimensions (Å)	a = 72.9, b = 48.2, c = 60.9	a = 72.7, b = 48.9, c = 61.1
	β = 107.0°	β = 106.7°
Resolution (Å)	20–1.8	30–1.8
(highest resolution shell)	(1.86–1.80)	(1.86–1.80)
Number of reflections		
Total	58,273	42,816
Unique	17,605	17,046
Completeness (%)[a]	93.3 (88.3)	90.6 (86.1)
I/σ	26.4 (11.0)	18.1 (3.3)
R_{sym} (%)	4.2 (9.3)	4.4 (33.7)
$R_{refinement}$ (%)	17.2	18.0
R_{free} (%)	20.6	23.3
B-factor (Å^2)		
Protein atoms	10.6	15.6
Nucleotide	11.8	14.4
Substrate/product	14.3/17.8 (AlF_3)	20.9
RMSDs		
Bond distances (Å)	0.007	0.007
Bond angles (°)	1.40	1.50

[a]Values in parenthesis are for the highest resolution shell.

tained 10 mM ADP, 4 mM $AlCl_3$, 40 mM NaF, and 10% 2-methyl-2,4-pentanediol (MPD). Similar conditions (5 mM $AlCl_3$ and 50 mM NaF) in solution result in moderate inhibition of the Mg^{2+}-activated enzyme (33% residual activity). Addition of 5 mM $AlCl_3$ or 50 mM NaF alone resulted in residual activities of 78 and 8%, respectively, suggesting that AlF_3 is less potent as inhibitor than fluoride ions. After about 40 min, a crystal was flash frozen and data was collected. The DTBS-MgADP-DTB-Pi complex was obtained by soaking the crystals overnight in a solution containing 10 mM DTB, 5 mM ADP, 5 mM Na_2HPO_4, 18% PEG 8000, 10 mM $Mg(CH_3COO)_2$, and 15% MPD at pH 6.4.

Diffraction data were collected on a Mar Research imaging plate mounted on a Rigaku rotating anode operating at 90 mA and 50 kV. All data were collected at 100K. X-ray data were processed and scaled with the Denzo and Scalepack software package (Otwinowski, 1993). Details of the data collection statistics are given in Table 1.

Model building and crystallographic refinement

The structures of the enzyme complexes were determined by difference Fourier methods using phases calculated from the refined model of the DTBS-MgADP-DAPA complex (Huang et al., 1995). In the calculation of the initial phases, the substrates and water molecules near the active site were excluded. The model of the protein was rebuilt to fit the initial map and then refined using the maximum likelihood algorithm in Refmac (Murshudov et al., 1997). Substrates/product molecules bound to the active site were then modeled into the difference electron densities using the program O (Jones et al., 1991). Additional rounds of refinement were done to model solvent molecules. During the whole refinement, 5% of the reflection data were excluded and used to monitor the *R*-free value. For details of refinement statistics, see Table 1. The protein models were analyzed with PROCHECK (Laskowski et al., 1993). The observed structure factor amplitudes and the atomic coordinates have been deposited with the Protein Data Bank, Brookhaven, accession codes 1bs1 for the DTBS-MgADP-DAPA-AlF_3 complex and 1dam for the DTBS-MgADP-DTB-Pi complex.

Acknowledgments

This work was supported by a grant from the Swedish Agricultural Research Council, the Swedish Natural Science Research Council and the Foundation for Strategic Research.

References

Alexeev D, Baxter RL, Sawyer L. 1994. Mechanistic implications and family relationships from the structure of dethiobiotin synthetase. *Structure 2*:1061–1072.

Alexeev D, Baxter RL, Smekal O, Sawyer L. 1995. Substrate binding and carboxylation by dethiobiotin synthetase: A kinetic and X-ray study. *Structure 3*:1207–1215.

Baldet P, Gerbling H, Axiotis S, Douce R. 1993. Biotin biosynthesis in higher plants. *Eur J Biochem 217*:479–485.

Baxter LR, Baxter HC. 1994. The mechanism of *Escherichia coli* dethiobiotin synthetase—The closure of the ureido ring of dethiobiotin involves formation of a carbamic-phosphate mixed anhydride. *J Chem Soc. Chem Commun*:759–760.

Coleman DE, Berghuis AM, Lee E, Linder ME, Gilman AG, Sprang SR. 1994. Structures of active conformations of Gia1 and the mechanism of GTP hydrolysis. *Science 265*:1405–1412

Eisenberg MA. 1973. Biotin: Biogenesis, transport and their regulation. *Adv Enzymol 38*:317–371.

Fischer AJ, Smith CA, Thoden JB, Smith R, Sutoh K, Holden HM, Rayment I. 1995. X-ray structures of the myosin motor domain of dictyostelium discoideum complexed with MgADP-BeFx and MgADP-AlF_4. *Biochemistry 34*:8960–8972.

Gibson KJ. 1997. Isolation and chemistry of the mixed anhydride intermediate in the reaction catalyzed by dethiobiotin synthetase. *Biochemistry 36*:8474–8478.

Gibson KJ, Lorimer GH, Rendina AR, Taylor WS, Cohen G, Gatenby AA, Payne WG, Roe DC, Lockett BA, Nudelman A, Marcovici D, Nachum A, Wexler BA, Marsilii EL, Turner IM Sr, Howe LD, Kalbach CE, Chi H. 1995. Dethiobiotin synthetase: The carbonylation of 7,8-diaminononanoic acid proceeds regiospecifically via the N7-carbamate. *Biochemistry 34*:10976–10984.

Gloeckler R, Ohsawa I, Speck D, Ledoux C, Bernard S, Zinsius M, Villeval D, Kisou T, Kamogawa K, Lemoine Y. 1990. Cloning and characterization of the *Bacillus sphaericus* genes controlling the bioconversion of pimelate into dethiobiotin. *Gene 87*:63–70.

Herron N, Thorn DL, Harlow RL, Davidson F. 1993. Organic action salts of the tetrafluoroaluminate anion. Yes, it does exist, and yes, it is tetrahedral. *J Am Chem Soc 115*:3028–3029.

Huang W, Jia J, Gibson KJ, Taylor WS, Rendina AR, Schneider G, Lindqvist Y. 1995. Mechanism of an ATP-dependent carboxylase, dethiobiotin synthetase, based on crystallographic studies of complexes with substrates and a reaction intermediate. *Biochemistry 34*:10985–10995.

Huang W, Lindqvist Y, Schneider G, Gibson KJ, Flint D, Lorimer G. 1994. Crystal structure of an ATP-dependent carboxylase, dethiobiotin synthetase, at 1.65 Å resolution. *Structure 2*:407–414.

Jones TA, Zou J, Cowan S, Kjeldgaard M. 1991. Improved methods for building protein models in electron density maps and location of errors in these models. *Acta Crystallogr A47*:110–119.

Käck H, Gibson KJ, Lindqvist Y, Schneider G. 1998. Snapshot of a phospholylated substrate intermediate by kinetic crystallography. *Proc Natl Acad Sci USA 95*:5495–5500.

Krell M, Eisenberg MA. 1970. The purification and properties of dethiobiotin synthetase. *J Biol Chem 245*:6558–6566.

Laskowski RA, McArthur MW, Moss DS, Thornton JM. 1993. Procheck: A program to check stereochemical quality of protein structures. *J Appl Crystallogr 26*:282–291.

Murshudov GN, Vagin AA, Dodson EJ. 1997. Refinement of macromolecular structures by the maximum-likelihood method. *Acta Crystallogr D53*:240–258.

Otwinowski Z. 1993. Data collection and processing. In: Sawyer L, Isaacs N, Bailey S, eds. *Proceeding of the CCP4 study weekend*. Daresbury Warrington, United Kingdom: SERC Laboratory. pp 56–62.

Scheffstek K, Ahmadian MR, Kabsch W, Wiesmüller L, Lautwein A, Schmitz F, Wittinghofer A. 1997. The Ras-RasGap complex: Structural basis for GTPase activation and its loss in oncogenic Ras mutants. *Science 277*:333–338.

Schlichting I, Reinstein J. 1997. Structures of active conformations of UMP kinase from *Dictyostelium dicoideum* suggest phosphoryl transfer is associative. *Biochemistry 36*:9290–9296.

Sondek DE, Lambright DG, Noel JP, Hamm HE, Sigler PB. 1994. GTPase mechanism of G proteins from the 1.7 Å crystal structure of transducing α-GDP-AlF_4^-. *Nature 372*:276–279.

Xu Y, Moréra S, Janin J, Cherfils J. 1997. AlF_3 mimics the transition state of protein phosphorylation in the crystal structure of nucleoside diphosphate kinase and MgADP. *Proc Natl Acad Sci USA 94*:3579–3583.

Yang G, Sandalova T, Lohman K, Lindqvist Y, Rendina A. 1997. Active site mutants of *Escherichia coli* dethiobiotin synthetase: Effects of mutations on enzyme catalytic and structural properties. *Biochemistry 36*:4751–4760.